Kinetics of the Reactions of Chlorinated Methyl Radicals (CH_2Cl, $CHCl_2$, and CCl_3) with NO_2 in the Temperature Range 220−360 K

Arkke J. Eskola, Wolf D. Geppert,[†] Matti P. Rissanen, Raimo S. Timonen,* and Lauri Halonen

Laboratory of Physical Chemistry, P.O. Box 55 (A.I. Virtasen aukio 1),
FIN-00014 University of Helsinki, Finland

Received: January 25, 2005; In Final Form: April 20, 2005

The kinetics of the reactions of chlorinated methyl radicals (CH_2Cl, $CHCl_2$, and CCl_3) with NO_2 have been studied in direct measurements at temperatures between 220 and 360 K using a tubular flow reactor coupled to a photoionization mass spectrometer. The radicals have been homogeneously generated at 193 or 248 nm by pulsed laser photolysis of appropriate precursors. Decays of radical concentrations have been monitored in time-resolved measurements to obtain the reaction rate coefficients under pseudo-first-order conditions with the amount of NO_2 being in large excess over radical concentrations. The bimolecular rate coefficients of all three reactions are independent of the bath gas (He or N_2) and pressure within the experimental range (1−6 Torr) and are found to depend on temperature as follows: $k(CH_2Cl + NO_2) = (2.16 \pm 0.08) \times 10^{-11} (T/300\ K)^{-1.12\pm0.24}$ cm^3 molecule^{-1} s^{-1} (220−363 K), $k(CHCl_2 + NO_2) = (8.90 \pm 0.16) \times 10^{-12} (T/300\ K)^{-1.48\pm0.13}$ cm^3 molecule^{-1} s^{-1} (220−363 K), and $k(CCl_3 + NO_2) = (3.35 \pm 0.10) \times 10^{-12} (T/300\ K)^{-2.2\pm0.4}$ cm^3 molecule^{-1} s^{-1} (298−363 K), with the uncertainties given as one-standard deviations. Estimated overall uncertainties in the measured bimolecular reaction rate coefficients are about ±25%. In the reactions $CH_2Cl + NO_2$, $CHCl_2 + NO_2$, and $CCl_3 + NO_2$, the products observed are formaldehyde, CHClO, and phosgene (CCl_2O), respectively. In addition, a weak signal for the HCl formation has been detected for the $CHCl_2 + NO_2$ reaction.

Introduction

Chlorinated hydrocarbon species such as CH_2Cl, $CHCl_2$, and CCl_3 radicals are important intermediates in combustion processes, especially during incineration of hazardous waste.[1] These species can be formed in unimolecular decomposition reactions of stable chlorinated hydrocarbon molecules under combustion conditions. Bond-breaking reactions for the stable chlorinated compounds occur uniformly at lower temperatures than for the hydrocarbons of similar size. Kinetic stability of the methyl radical increases in the combustion environment as one or more hydrogen atoms in the radical are substituted by chlorine atoms, because peroxy adducts formed via radical addition to O_2 increasingly favor decomposition back to the radical and O_2 as chlorine substitution increases.[2] This is due to the weaker C−O bond in the chlorinated peroxy adducts than in their hydrocarbon counterparts, thus increasing the importance of reactions of chlorinated methyl radicals with species other than molecular oxygen. Reactions with NO_2 can be expected to be important during the oxidation of chlorinated compounds at low temperatures, because traces of nitrogen oxides are also often present.[3] In addition, the chlorinated hydrocarbons increase soot formation in fuel-rich oxidation.[4]

In the present work, we describe first direct experimental studies for reactions 1−3.

$$CH_2Cl + NO_2 \rightarrow \text{products} \qquad (1)$$

$$CHCl_2 + NO_2 \rightarrow \text{products} \qquad (2)$$

$$CCl_3 + NO_2 \rightarrow \text{products} \qquad (3)$$

Investigating these kinds of series of reactions does not only give specific kinetic parameters in individual cases but it also makes ground for the theoreticians to gain deeper mechanistic understanding and, probably, to reveal whether a general trend can be found to explain the reactivity of these and similar radicals with NO_2.[5]

The number of the substituted methyl radical reactions with NO_2 subjected to direct studies is few. Nesbitt et al.[6] have investigated the reaction of hydroxymethyl radical (CH_2OH) with NO_2 at low pressures (~1 Torr He) using a discharge-flow system combined with a mass spectrometer and obtained a bimolecular rate coefficient $(8.3 \pm 2.1) \times 10^{-12}$ cm^{-3} s^{-1} at room temperature. Pagsberg et al.[7] have studied the same reaction at room temperature and atmospheric pressure obtaining a rate coefficient $(2.3 \pm 0.4) \times 10^{-11}$ cm^{-3} s^{-1} using pulse radiolysis to generate radicals and UV-absoption to measure the kinetics. They also observed the formation of a long-lived or stable product. Combining this finding with their larger rate coefficient at atmospheric pressure, they concluded that the difference between the two rate coefficient values is probably due to the effect of bath gas pressure on stabilizing the adducts. The $CF_3 + NO_2$ reaction has been studied extensively (see ref 8 and references therein), in contrast to the other substituted

---

* To whom correspondence should be addressed. E-mail: raimo.timonen@helsinki.fi.

[†] Current address: Department of Molecular Physics, Alba Nova, University of Stockholm, Roslagstullbacken 21, S-10691 Stockholm, Sweden.

10.1021/jp050441a CCC: $30.25

methyl radical reactions with NO_2. Breheny et al.[8] have investigated the $CF_3 + NO_2$ reaction at room temperature and over the pressure range 1.5−110 Torr of Ar and N_2 using time-resolved infrared emission spectroscopy obtaining a bimolecular rate coefficient $(1.75 \pm 0.26) \times 10^{-11}$ cm^{-3} s^{-1}. Their results with previous work[9] indicate that the main channel produces FNO and CF_2O products, though at higher pressures, the formation of the adduct might have some minor importance.[8] Slagle et al.[10] have studied the $CF_2Cl + NO_2$ reaction at room temperature and at low pressure (∼1 Torr He) obtaining the rate coefficient $(9.6 \pm 1.9) \times 10^{-12}$ cm^{-3} s^{-1} using a flow reactor combined with a photoionization mass spectrometer. No previous experimental data on the temperature dependences of the substituted methyl radical reactions with NO_2 subject to direct studies are available.

Experimental

Details of the experimental apparatus and procedures used have been described previously,[11] so only a brief overview is given here. The gas mixture flowing through a tubular reactor contained the radical precursor (<0.15%), NO_2 in varying amounts, and an inert carrier gas (He or N_2) in large excess (>99.7%). The CH_2Cl, $CHCl_2$, and CCl_3 radicals were homogeneously generated from appropriate precursors at 193 or 248 nm by pulsed unfocused exciplex laser (ELI-76E) photolysis along the flow reactor. Gas flow velocity through the tubular, temperature-controlled reactor was about 5 m s^{-1}, which ensured that the gas mixture was completely replaced between laser pulses with the repetition rate of 5 Hz. The employed reactor tubes with 6-, 8-, and 17-mm inner diameters (id) were made of seamless stainless steel and were coated with halocarbon wax.

The gas mixture was continuously sampled through a 0.4-mm diameter hole at the side of the reactor and was formed into a beam by a conical skimmer before it entered into a vacuum chamber containing a photoionization mass spectrometer (PIMS). As the gas beam traversed the ion source, a portion was photoionized and the ions formed were mass selected in a quadrupole mass spectrometer (Extrel, C-50/150-QC/19 mm rods). Ionization radiation in the PIMS was provided by atomic resonance lamps: a Cl-lamp (8.9−9.1 eV) for CH_2Cl, $CHCl_2$, and CCl_3, a H-lamp (10.2 eV) for CH_2Cl, $CHCl_2$, CCl_3, CH_2ClO, $CHCl_2O$, CCl_3O, CH_2ClONO_2, CH_2ClNO_2, CCl_3NO_2, HNO, CClO, and NO, an Ar-lamp (11.6−11.8 eV) for CD_2O, and a Ne-lamp (16.7−16.9 eV) for HCl, HNO_2, ClO, CH_2ClO, CHClO, CCl_3NO_2, ClNO, and CCl_2O. The title radical decays were mainly measured with the Cl-lamp, while a few profiles were obtained with the H-lamp. However, no differences in profiles were observed. Temporal ion signals were recorded by a multichannel scaler (EG&G Ortec MCS plus) from 10 ms before each laser pulse up to 80 ms following the pulse. Typically, a profile from 3000 to 15000 repetitions was accumulated before the nonlinear least-squares method was used to fit the data to an exponential function, $[R]_t = [R]_0 \times \exp(-k't)$, where $[R]_t$ is the signal proportional to the radical concentration at time t and k' is the first-order rate coefficient.

The CH_2Cl radicals were generated either from CH_2ClBr[12] as

$$CH_2ClBr + h\nu(193\text{ nm}) \rightarrow CH_2Cl + Br \tag{4a}$$

$$\rightarrow \text{other products} \tag{4b}$$

or from CH_2Cl_2 (CD_2Cl_2)[13] as

$$CH_2Cl_2\ (CD_2Cl_2) + h\nu(193\text{ nm}) \rightarrow CH_2Cl\ (CD_2Cl) + Cl \tag{5a}$$

$$\rightarrow \text{other products} \tag{5b}$$

Deuterated dichloromethane (CD_2Cl_2) was used as a precursor instead of CH_2ClBr or CH_2Cl_2 to avoid contributions from NO (m = 30 u, IE (ionization energy) = 9.26 eV),[14] when the formation of the formaldehyde product ($m(CH_2O) = 30$ u, $m(CD_2O) = 32$ u, and IE ≈ 10.9 eV for both)[14] was measured. The $CHCl_2$ radicals were produced either from $CHCl_3$[13] as

$$CHCl_3 + h\nu(193\text{ nm}) \rightarrow CHCl_2 + Cl \tag{6a}$$

$$\rightarrow \text{other products} \tag{6b}$$

or from $CHCl_2Br$[15] as

$$CHCl_2Br + h\nu(248\text{ nm}) \rightarrow CHCl_2 + Br \tag{7a}$$

$$\rightarrow \text{other products} \tag{7b}$$

The CCl_3 radicals were generated from CCl_3Br[16] as

$$CCl_3Br + h\nu(248\text{ nm}) \rightarrow CCl_3 + Br \tag{8}$$

As mentioned, the radicals were produced by both 193- and 248-nm laser photolysis from different precursors to ensure that the possible extra internal energy of the produced species would vary for the different measurements. In comparison of the results of these measurements, no difference was obtained because of the precursor or wavelength change. Similar tests have been performed previously, for example, by Timonen[17] and Krasnoperov et al.,[18] with the same conclusion.

Formaldehyde (or CD_2O when CD_2Cl_2 was used as a precursor) was detected as a product for the reaction of the CH_2Cl/CD_2Cl radical with NO_2. Formation of NO was also measured, but because of the production of radicals other than CH_2Cl (CD_2Cl) in the photolysis or in the secondary chemistry and their possible reactions with NO_2 to produce NO, it was impossible to assign the origin of NO unambiguously to the CH_2Cl (CD_2Cl) + NO_2 reaction. Other potential products that were searched for but not detected for this reaction include CH_2ClO, CH_2ClONO_2, CH_2ClNO_2, HNO, HNO_2, and HCl. For the reaction of the $CHCl_2$ radical with NO_2, the detected product was CHClO ($CHCl_2Br$ was used as a precursor) as well as NO, whose origin was also difficult to assign quantitatively in this case. A weak signal was also measured for the formation of HCl. Other potential products that were searched for but not detected include $CHCl_2O$, HNO, and HNO_2. The detected product of the reaction of the CCl_3 radical with NO_2 was CCl_2O. The measured signal for the NO formation was weak and included a small portion from the photodissociation of the reactant NO_2. For the $CCl_3 + NO_2$ reaction, other potential products that were searched for but not detected include CCl_3O, CCl_3NO_2, CClO, and ClNO. When the formaldehyde or chlorinated formaldehyde was observed and assigned to the product of reactions 1−3, it was also confirmed that no other radicals were formed in the photolysis or in the secondary reactions that could have produced this primary product.

Radical precursors, CH_2Cl_2 (Mallinckrodt, purity > 99%), CD_2Cl_2 (Aldrich, purity > 99%), CH_2ClBr (Fluka, purity ≥ 98%), $CHCl_3$ (Rathburn, purity > 99%), $CHCl_2Br$ (Aldrich, purity > 98%), CCl_3Br (Aldrich, purity 99%), and NO_2 (Merck, purity 98%), were degassed before use. The NO_2 gas was diluted in He to form a 10% mixture and was stored in a blackened glass bulb. Helium (Messer-Griesheim purity of 99.9996%) and nitrogen (Aga purity of 99.9999%) were employed as supplied.

Results and Discussion

The decay of R (R = CH_2Cl, $CHCl_2$, or CCl_3) was first monitored in time-resolved experiments without NO_2 to obtain the wall reaction rate coefficient, k_{wall}, which was measured by reducing precursor concentration or laser intensity until the rate obtained for this process no longer depended on these factors and an exponential fit to the temporal ion signal showed no deviation from a first-order decay. When these conditions were achieved, it was presumed that all radical−radical processes were suppressed (i.e., these had negligible rates compared to the first-order processes occurring in the system). Initial R concentrations were then typically below 3×10^{11} molecules cm^{-3}, which were estimated from the laser fluences and the known absorption cross sections of the precursor at used wavelengths. Experiments were mainly performed with relatively high precursor concentration ($\sim 10^{13}-10^{14}$ molecules cm^{-3}) but with low laser intensity to minimize NO_2 decomposition. A few measurements were carried out with low precursor concentration and high laser intensity to test the possible importance of radical−precursor reactions. It was found that changes in precursor concentration had a minor or no effect on k_{wall} and no effect on $k(R + NO_2)$.

The first-order rate coefficient (k') was measured as a function of the NO_2 concentration ($[NO_2]$), which was always much higher (>15 times) than [R], resulting in pseudo-first-order reaction kinetics. Since the only significant processes consuming R during these experiments were the reaction with NO_2 and k_{wall}, the bimolecular reaction rate coefficient $k(R + NO_2)$ could be obtained from the slope of the k' versus $[NO_2]$ plot. A typical example is shown in Figure 1 for the $CH_2Cl + NO_2$ reaction with the CH_2Cl radical signal decay inserted in the upper left corner. In the lower right corner, both the CD_2Cl radical signal decay and the product (CD_2O) formation profile are also shown, when CD_2Cl_2 was used as a precursor instead of CH_2Cl_2 under similar conditions to avoid complications because of the NO (m/z (mass versus charge number ratio) = 30 u) formation at the same m/z ratio as CH_2O (m/z = 30 u). In addition, no secondary kinetic isotope effect ($k(CD_2Cl + NO_2)/k(CH_2Cl + NO_2)$) was observed above the experimental uncertainty (Table 1, g).

As noted, for the $CH_2Cl + NO_2$, $CHCl_2 + NO_2$, and $CCl_3 + NO_2$ reactions, the products observed are formaldehyde, CHClO, and phosgene (CCl_2O), respectively. In addition, a weak signal for the HCl formation has been detected for the $CHCl_2 + NO_2$ reaction. In these cases, the growth time of the product matched that of the R decay in the reaction with NO_2. In addition, several other potential products were searched. The absence of a measurable ion signal in these cases cannot be taken as a proof of the insignificance of these possible products in reactions 1−3 because the sensitivity of our experimental system is not known for these species.

As mentioned in the Introduction, Breheny et al.[8] have investigated the $CF_3 + NO_2$ reaction at room temperature, and their results indicate that the main channel produces CF_2O and FNO products, though at higher pressures the formation of the adduct might have some minor importance. Similar reaction channels could also be expected in the studied reactions. However, it is impossible to propose exact mechanisms for the current reactions, since we are unable to firmly identify all the possible products, as mentioned above.

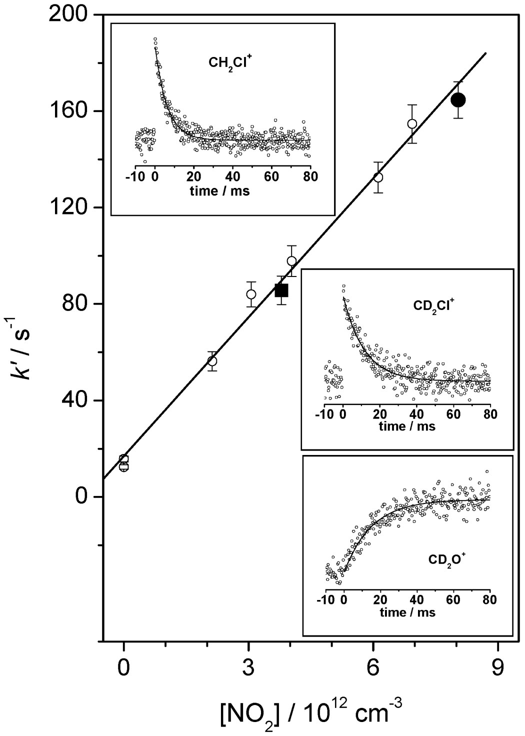

Figure 1. Plot of the first-order CH_2Cl rate coefficient k' vs $[NO_2]$ at $T = 298$ K and $P = 5$ Torr in an 8-mm id reactor tube. The insert in the upper left corner shows the ion signal profile for the CH_2Cl decay under the conditions of the solid circle in the plot: $[NO_2] = 8.0 \times 10^{12}$ molecule cm^{-3}, $k'_{decay}(CH_2Cl) = 164 \pm 8\ s^{-1}$, and $k_{wall} = 13 \pm 2\ s^{-1}$. The inserts in the lower right corner show the ion signal profile for the CD_2Cl radical signal decay and product (CD_2O) formation under the conditions of the solid square in the plot, when CD_2Cl_2 was used as a precursor instead of CH_2Cl_2 to avoid complications from the NO formation. Conditions were otherwise similar and $[NO_2] = 3.8 \times 10^{12}$ molecule cm^{-3}. Uncertainties are one-standard deviations (1σ).

Some NO_2 was photolyzed in the laser pulse at 193 or 248 nm according to the following reactions:[19,20]

$$NO_2 + h\nu(193\ \text{nm}) \rightarrow NO + 0.55\ O(^1D) + 0.45\ O(^3P) \quad (9)$$

$$NO_2 + h\nu(248\ \text{nm}) \rightarrow NO + O(^3P) \quad (10)$$

Oxygen atom concentration was suppressed using low laser intensity and high appropriate precursor concentration. It was typically in the range $0.6-3 \times 10^{10}$ molecule cm^{-3}, which was estimated from the absorption cross section[19,20] and the measured laser intensity. Experiments performed with higher laser intensity and lower precursor concentration yielded essentially the same values within the experimental uncertainty for the bimolecular rate coefficients. Measurements performed using either N_2 or He as buffer gas yielded the same bimolecular reaction rate constants within experimental error, which rules out any important effects caused by excited oxygen atoms [$O(^1D)$] on kinetics, because under experimental conditions nitrogen quenches them already within the first 10 μs after photolysis pulse.

The equilibrium between NO_2 and N_2O_4 is shifted toward the dimer at low temperatures ($T \leq 220$ K).[21] However, in our system, the amount of NO_2 converted to N_2O_4 was insignificant (<0.1%) because of the low NO_2 concentrations used and because of the small value of the equilibrium coefficient at room temperature. In addition, equilibrium was not reached within the short residence time (∼100 ms) in the cooled zone of the reactor because the recombination rate for dimer formation ($k' \approx 0.05\ s^{-1}$) is slow under experimental conditions.[22] Such

TABLE 1: Results and Conditions of the Experiments[a] Used To Measure the Bimolecular Rate Coefficients of the Reaction $R + NO_2 \rightarrow$ Products[i]

T/K	P^b/Torr	$10^{-12}[NO_2]$/cm^{-3}	$d^c_{reactor}$/mm	k_{wall}/s^{-1}	$10^{12}k^d$/cm^3 s^{-1}
$R = CH_2Cl$					
$k(CH_2Cl + NO_2) = (2.16 \pm 0.08) \times 10^{-11} \times (T/300\ K)^{-1.12\pm0.24}$ cm^3 s^{-1}					
220	2.2	1.2−4.7	17	16	31.7 ± 1.4
242[e]	3.0	2.5−8.5	6	18	23.0 ± 1.0
241	2.2	1.2−5.6	17	11	31.2 ± 1.1
241	4.0	1.8−5.8	8	13	26.2 ± 1.4
267	5.2	1.8−7.6	8	11	22.2 ± 0.5
267	2.7	1.8−5.3	17	7	29.4 ± 0.6
298	1.0	1.6−6.9	17	5	20.4 ± 0.8
298	1.1[f]	1.7−7.9	17	10	21.9 ± 1.5
298	5.0	1.9−7.3	8	7	19.7 ± 0.6
298	3.0	1.2−7.8	17	8	25.5 ± 1.0
298	3.0	1.9−7.8	17	6	24.4 ± 0.5
298[g]	5.1	2.0−5.6	8	10	23.4 ± 0.3
298[e]	5.0	2.1−8.0	8	13	19.2 ± 0.7
336	3.0	1.7−8.0	17	7	20.8 ± 0.6
363	6.0	2.0−9.2	8	8	16.2 ± 0.2
$R = CHCl_2$					
$k(CHCl_2 + NO_2) = (8.90 \pm 0.16) \times 10^{-12} \times (T/300\ K)^{-1.48\pm0.13}$ cm^3 s^{-1}					
220[h]	2.6	6.7−27.7	6	19	13.4 ± 0.5
241	2.2	2.0−14.5	17	6	12.9 ± 0.6
241	4.1	2.5−18.9	8	8	11.3 ± 0.4
242[h]	2.6	6.1−29.4	6	21	12.6 ± 0.6
266[h]	6.0	7.4−24.2	6	12	12.5 ± 0.5
266	4.5	2.4−22.0	8	6	10.5 ± 0.4
298	1.0	4.4−21.8	17	2	9.09 ± 0.3
298[h]	1.9[f]	6.1−29.0	6	17	9.39 ± 0.4
298	2.5	4.5−27.7	17	3	9.41 ± 0.6
298[h]	3.0	6.5−33.3	6	16	8.31 ± 0.4
298	4.9	3.8−17.8	8	5	8.40 ± 0.7
298[h]	5.9	7.6−37.1	6	15	8.89 ± 0.6
336[h]	5.9	9.2−38.3	6	12	7.30 ± 0.2
336	6.3	4.5−20.6	8	7	7.65 ± 0.6
363	6.2	4.4−18.2	8	8	6.66 ± 0.3
$R = CCl_3$					
$k(CCl_3 + NO_2) = (3.35 \pm 0.10) \times 10^{-12} \times (T/300\ K)^{-2.2\pm0.4}$ cm^3 s^{-1}					
298	1.0	13.2−46.9	17	0	3.54 ± 0.17
298	2.5	13.6−60.1	17	0	3.71 ± 0.12
298	2.5	9.8−46.0	8	2	2.94 ± 0.10
298	5.0	9.5−46.9	8	1	3.34 ± 0.12
298	2.1[f]	10.6−52.9	8	4	3.46 ± 0.13
318	2.0	7.9−34.5	17	0	2.91 ± 0.09
336	5.7	10.1−53.4	8	2	2.71 ± 0.05
363	6.2	9.3−46.5	8	4	2.14 ± 0.05

[a] Range of precursor concentrations used: $(1.2-9.4) \times 10^{13}$ molecule cm^{-3} for CH_2ClBr, $(6.3-21.9) \times 10^{13}$ molecule cm^{-3} for $CH_2Cl_2(CD_2Cl_2)$, $(2.1-7.2) \times 10^{13}$ molecule cm^{-3} for $CHCl_2Br$, $(0.3-9.7) \times 10^{13}$ molecule cm^{-3} for $CHCl_3$, and $(1.5-6.62) \times 10^{13}$ molecule cm^{-3} for CCl_3Br. Laser intensities used were 2−23 mJ/cm^2 (193 nm) and 7−34 mJ/cm^2 (248 nm). Estimated initial radical concentrations $0.4-4.2 \times 10^{11}$ molecule cm^{-3}. [b] Helium used as a buffer gas unless otherwise stated. [c] Reactor inner diameter. Coated with halocarbon wax. [d] Statistical uncertainties shown are 1σ; estimated overall uncertainty is ±25%. [e] CH_2Cl_2 used as a precursor. [f] Nitrogen used as a buffer gas. [g] CD_2Cl_2 used as a precursor. [h] $CHCl_3$ used as a precursor. [i] $R = CH_2Cl$, $CHCl_2$, and CCl_3.

a small amount of dimer does not have any significant effect on our results.

Investigations were also performed to find out the possible presence of second-order R ($R = CH_2Cl$, $CHCl_2$, or CCl_3 radical) heterogeneous wall reactions. Both small (6 or 8 mm) and large (17 mm) id reactor tubes with the same coatings were employed to vary the surface-to-volume ratio (almost with a factor of 3).[11,23] One would expect a larger bimolecular reaction rate coefficient $k(R + NO_2)$ for the small than for the large tube, if second-order heterogeneous reactions occurred in any significant extent. This was not observed and only the first-order wall reaction rate coefficient k_{wall} was larger for the small than for the large tube. We concluded that second-order wall reactions are unimportant in our experiments.

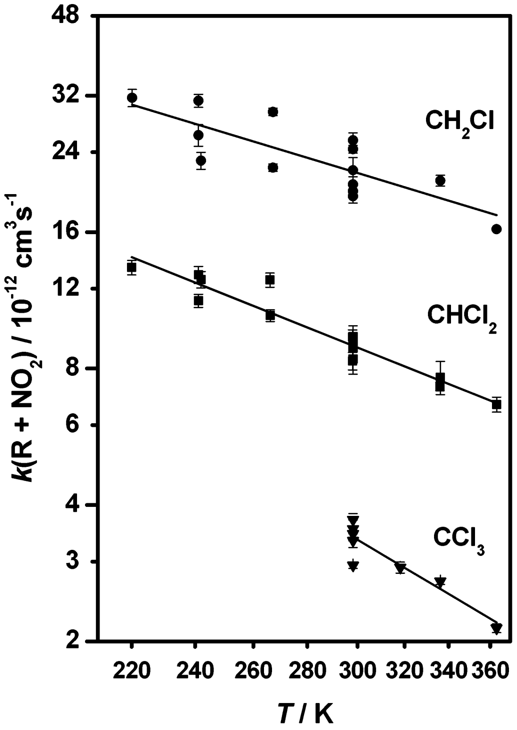

Figure 2. Double-logarithmic plots of the measured bimolecular rate coefficients versus T.

The measured bimolecular reaction rate coefficients for the CH_2Cl, $CHCl_2$, and CCl_3 radical reactions with NO_2 are shown in Table 1 with their statistical uncertainties (1σ) and experimental conditions. Estimated overall uncertainties in measured bimolecular reaction rate coefficients are about ±25%. These arise mainly from the uncertainties in determining reactant concentrations and from the uncertainties in decay rate coefficients. Linear least-squares fits to an expression $k = A \times (T/300\ K)^n$, where T is temperature in K and A and n are empirical parameters, are given in Table 1. Double-logarithmic plots of the bimolecular rate coefficients for the CH_2Cl, $CHCl_2$, and CCl_3 radical reactions with NO_2 are shown in Figure 2.

Measurements were carried out at different pressures to investigate possible contributions of three-body processes. Changes of the pressure between 1 and 5 Torr (He) did not change the rates in any of the $R + NO_2$ reactions studied. Therefore, no fast three-body processes are likely to be present in any significant extent in these systems. This is consistent with the abovementioned observations on the $CF_3 + NO_2$ reaction[8] but is different from a recent study by Wollenhaupt et al.[24] on the $CH_3 + NO_2$ reaction, where both bimolecular and termolecular reaction channels were observed. According to that study, there is an increase of about 40% in the reaction rate coefficient at room temperature as the pressure is changed near the low-pressure limit of the termolecular component from 1 to 5 Torr. If similar or larger pressure dependencies had occurred in the current reactions studied, this should have been observed. On the other hand, Cumming et al.[25] have studied the kinetics of the $CCl_3 + NO_2$ reaction by following the buildup of CCl_3NO_2 at 290 nm using the pulsed radiolysis UV-absoption method. Measurements were performed at room temperature and in the pressure range about 100−1500 Torr. Within this range, the buildup of CCl_3NO_2 was linearly proportional to Ar pressure, and the termolecular rate coefficient determined was $k(300\ K) = 3.31 \times 10^{-31}$ cm^6 s^{-1}. Using this value to estimate the reaction rate coefficient at 5 Torr for this termolecular channel gives $k(300\ \mathrm{K}) = 5.3 \times 10^{-14}\ \mathrm{cm^3\ s^{-1}}$, which is only about 1.5% from the bimolecular reaction rate coefficient $k(300\ \mathrm{K}) = 3.35 \times 10^{-12}\ \mathrm{cm^3\ s^{-1}}$ measured in the current study. However, at atmospheric pressure, the termolecular channel gives $k(300\ \mathrm{K}) = 8.0 \times 10^{-12}\ \mathrm{cm^3\ s^{-1}}$, which is more than twice as high as the current bimolecular reaction rate coefficient. We conclude that under conditions employed in this work the contribution of the possible termolecular channel is negligible.

A comparison on the effect of chlorination in the reactions of the CH_3, CH_2Cl, $CHCl_2$, and CCl_3 radicals with NO_2 can be made using current experimental data. It is interesting to observe a clear trend from the CH_2Cl to the CCl_3 radical as reactivity at room temperature decreases at each step about 60% after the hydrogen atom substitution by the chlorine atom. However, this apparent conclusion does not apply to the methyl radical, because the bimolecular reaction rate coefficient of the $CH_3 + NO_2$ reaction[26] [$k(295\mathrm{K}) = 2.5 \times 10^{-11}\ \mathrm{cm^3\ s^{-1}}$] is close to the current value of the $CH_2Cl + NO_2$ reaction [$k(300\ \mathrm{K}) = 2.16 \times 10^{-11}\ \mathrm{cm^3\ s^{-1}}$].

There exists now enough information on the kinetics of reactions of polyatomic free radicals with NO_2 to start to search linear relationships with different properties to account for the observed reactivity differences. Several experimental studies indicate that reactivity in homologous series of radical/molecule reactions correlates with the ionization potential (*IP*) of the species that is electron-donating in the transition state and with the electron affinity (*EA*) of the electron-withdrawing species.[5,29,30] For example, Paltenghi et al.[30] have obtained a good linear relationship for the alkyl radical reactions with O_2 and O_3 by plotting $\log(k_{300\mathrm{K}})$ versus $IP(\mathrm{R}) - EA(\mathrm{O_2}\ \text{or}\ \mathrm{O_3})$. Consequently, we first plotted $\log(k_{300\mathrm{K}})$ versus $IP(\mathrm{R}) - EA(\mathrm{NO_2})$. However, no clear correlation was observed in our case. Instead, linear relationship was obtained when $\log(k_{300\mathrm{K}})$ versus $EA(\mathrm{R})$ was plotted [$IP(\mathrm{NO_2})$ is a constant in this plot and was omitted for simplicity], which is shown in Figure 3 for several substituted methyl radicals (CH_3, C_2H_5, CH_2CN, CF_3, and CF_2Cl) in addition to current results. A few other radicals (C_2H_3, C_3H_3, C_3H_5, and CH_3CO) are also included for comparison. In addition to the clear correlation in the case of substituted methyl radicals shown in Figure 3, it is interesting to note that the reactivity of the radicals with NO_2 decreases as their electron affinity increases. A similar behavior has been observed previously for the $R + Br_2$[31] and $R + Cl_2$[32] reactions, where R is a substituted methyl radical. Deviations from the $\log(k_{300\mathrm{K}})$ versus $IP - EA$ relationship have been observed for the OH and H radicals in their reactions with halogenated ethenes.[5,33]

In line with our previous studies on the $C_2H_3 + NO_2$ and $C_3H_3 + NO_2$ systems,[35] no evidence of an activation barrier was observed in any of the present reactions. Instead, comparing the temperature dependencies of the $R + NO_2$ reactions ($R = C_2H_3$, C_3H_3, CH_2Cl, $CHCl_2$, and CCl_3), it is seen among these systems that, when the reaction becomes slower, the n-parameter in $T^{\,n}$ becomes more negative, that is, shows increasingly negative temperature dependency: $C_2H_3 + NO_2$ [$k_{300\mathrm{K}} = 4.19 \times 10^{-11}\ \mathrm{cm^3\ s^{-1}}$, $k \propto T^{-0.6}$], $C_3H_3 + NO_2$ [$k_{300\mathrm{K}} = 2.55 \times 10^{-11}\ \mathrm{cm^3\ s^{-1}}$, $k \propto T^{-1.06}$], $CH_2Cl + NO_2$ [$k_{300\mathrm{K}} = 2.16 \times 10^{-11}\ \mathrm{cm^3\ s^{-1}}$, $k \propto T^{-1.12}$], $CHCl_2 + NO_2$ [$k_{300\mathrm{K}} = 0.89 \times 10^{-11}\ \mathrm{cm^3\ s^{-1}}$, $k \propto T^{-1.48}$], and $CCl_3 + NO_2$ [$k_{300\mathrm{K}} = 0.34 \times 10^{-11}\ \mathrm{cm^3\ s^{-1}}$, $k \propto T^{-2.2}$]. However, the temperature dependence of the $CCl_3 + NO_2$ system is less well determined than in the case of other reactions because of the limited experimental temperature range. Theoretical studies have concluded that negative temperature dependency for the elementary reaction having no potential energy barrier along the reaction coordinate should not possess the n-parameter in $T^{\,n}$ more negative than -0.5, if the reaction rate is independent from the degree of internal excitation of the reactants.[36] Combining this with the current results, it could be concluded that either the reaction rates considered depend on the internal energies of the reactants or, alternatively, a weakly bound complex is formed.[37] This intermediate could either dissociate to reform the original reactants or rearrange to produce the final products.[38] Additional kinetic studies are in progress to improve our understandings on the reactivity of halogenated alkyl radicals.

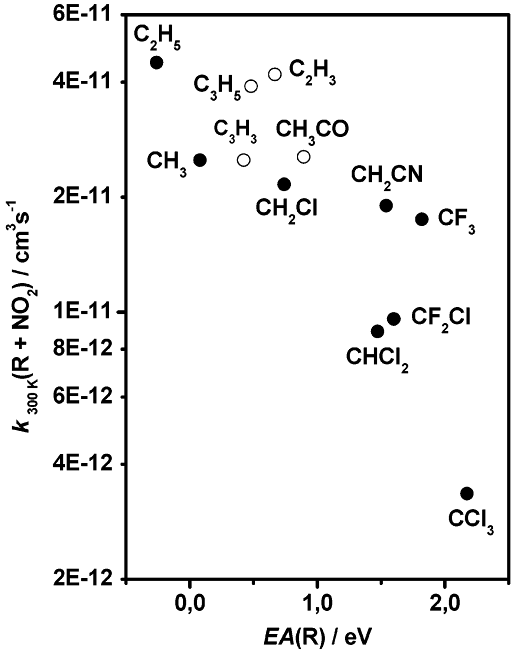

Figure 3. A plot of $R + NO_2$ reaction rate constants vs adiabatic EA(R) at 300 K involving substituted methyl radicals (CH_3,[26] C_2H_5,[27] CH_2CN,[27] CF_3,[8] and CF_2Cl[10]) shown in filled circles including current results. A few other radicals (C_2H_3,[35] C_3H_3,[35] C_3H_5,[28] and CH_3CO[10]) are also shown as open circles for comparison. Values for the radical adiabatic electron affinities are taken from ref 14 except for C_3H_3, which is taken from ref 34.

Conclusions

Bimolecular rate coefficients of the $CH_2Cl + NO_2$, $CHCl_2 + NO_2$, and $CCl_3 + NO_2$ reactions have been measured and have been found to obey the following temperature dependence: $k(\mathrm{CH_2Cl + NO_2}) = (2.16 \pm 0.08) \times 10^{-11}\ (T/300\ \mathrm{K})^{-1.12\pm0.24}\ \mathrm{cm^3\ molecule^{-1}\ s^{-1}}$, $k(\mathrm{CHCl_2 + NO_2}) = (8.90 \pm 0.16) \times 10^{-12}\ (T/300\ \mathrm{K})^{-1.48\pm0.13}\ \mathrm{cm^3\ molecule^{-1}\ s^{-1}}$, and $k(\mathrm{CCl_3 + NO_2}) = (3.35 \pm 0.10) \times 10^{-12}\ (T/300\ \mathrm{K})^{-2.2\pm0.4}\ \mathrm{cm^3\ molecule^{-1}\ s^{-1}}$. The absence of bath gas pressure dependence of the reaction rates rules out the importance of three-body processes in these systems. Formaldehyde (CD_2O) has been detected as a product for the $CH_2Cl(CD_2Cl) + NO_2$ reaction. In the case of the $CHCl_2 + NO_2$ reaction, CHClO is the main product with weak signal from the HCl formation. Phosgene (CCl_2O) has been detected as a product for the $CCl_3 + NO_2$ reaction. There is no experimental evidence on an activation barrier for any of the reactions studied.

Acknowledgment. A.J.E. thanks the KONE foundation for research grants. W.D.G. acknowledges support from a TMR fellowship under the “Improving Human Potential and the

Socio-economic Knowledge Database" program of the European Union (contract number HPRN-CT-2000-00022). R.S.T. also acknowledges support from the Bioscience and Environmental Research Council of the Academy of Finland and Maj and Tor Nessling Foundation. L.H. thanks the Natural Science and Engineering Research Council of the Academy of Finland for financial support.

References and Notes

(1) Tsang, W. *Combust. Sci. Technol.* **1990**, *74*, 99.

(2) Knyazev, V. D.; Slagle I. R. *J. Phys. Chem. A* **1998**, *102*, 1770.

(3) Faravelli, T.; Frassoldati, A.; Ranzi, E. *Combust. Flame* **2003**, *132*, 188.

(4) Violi, A.; D'Anna, A.; D'Alessio, A. *Chemosphere* **2001**, *42*, 463.

(5) Donahue, N. M. *Chem. Rev.* **2003**, *103*, 4593.

(6) Nesbitt, F. L.; Payne, W. A.; Stief, L. J. *J. Phys. Chem.* **1989**, *93*, 5158.

(7) Pagsberg, P.; Munk, J.; Anastasi, C.; Simpson, V. J. *J. Phys. Chem.* **1989**, *93*, 5162.

(8) Breheny, C.; Hancock, G.; Morrell, C. *Phys. Chem. Chem. Phys.* **2000**, *2*, 5105.

(9) Pagsberg, P.; Jodkowski, J. T.; Ratajczak, E.; Sillesen, A. *Chem. Phys. Lett.* **1998**, *286*, 138.

(10) Slagle, I. R.; Gutman, D. *J. Am. Chem. Soc*. **1982**, *104*, 4741.

(11) Eskola, A. J.; Timonen, R. S. *Phys. Chem. Chem. Phys.* **2003**, *5*, 2557.

(12) (a) Orkin, V. L.; Khamaganov, V. G.; Guschin, A. G.; Huie, R. E.; Kurylo, M. J. *J. Phys. Chem. A* **1997**, *101*, 174. (b) Tzeng, W. B.; Lee, Y. R.; Lin, S. M. *Chem. Phys. Lett.* **1994**, *227*, 467.

(13) Brownsword, R. A.; Hillenkamp, M.; Laurent, T.; Vatsa, R. K.; Volpp, H.-R.; Wolfrum, J. *J. Phys. Chem. A* **1997**, *101*, 5222.

(14) *NIST Chemistry WebBook, NIST Standard Reference Database Number 69*; Linstrom, P. J., Mallard, W. G., Eds.; National Institute of Standards and Technology: Gaithersburg, MD, Mar 2005 (http://webbook.nist.gov).

(15) Bilde, M.; Wallington, T. J.; Ferronato, C.; Orlando, J. J.; Tyndall, G. S.; Estupiñan, E.; Haberkorn, S. *J. Phys. Chem. A* **1998**, *102*, 1976.

(16) (a) Luther, K.; Oum, K.; Troe, J. *J. Phys. Chem. A* **2001**, *105*, 5535. (b) Lee, Y. R.; Tzeng, W. B.; Yang, Y. J.; Lin, Y. Y.; Lin, S. M. *Chem. Phys. Lett.* **1994**, *222*, 141.

(17) Timonen, R. *Ann. Acad. Sci. Fenn. Ser. A2* **1988**, *218*, 5.

(18) Krasnoperov, L. N.; Mehta, K. *J. Phys. Chem. A* **1999**, *103*, 8008.

(19) Sun, F.; Glass, G. P.; Curl, R. F. *Chem. Phys. Lett.* **2001**, *337*, 72.

(20) Atkinson, R.; Baulch, D. L.; Cox, R. A.; Hampson, R. F., Jr.; Kerr, J. A.; Troe, J. *J. Phys. Chem. Ref. Data* **1992**, *21*, 1125.

(21) Harwood: M. H.; Jones, R. L. *J. Geophys. Res.* **1994**, *99*, 22955.

(22) Borrell, P.; Cobos, C. J.; Luther, K. *J. Phys. Chem.* **1988**, *92*, 4377.

(23) Kaufman, F. *Progress in Reaction Kinetics*; Porter, G., Ed.; Pergamon: New York, **1961**, *1*, 1.

(24) Wollenhaupt, M.; Crowley, J. N. *J. Phys. Chem. A* **2000**, *104*, 6429.

(25) Cumming, J. B.; Cooper, R.; Mulac, W. A.; Gordon, S. *Radiat. Phys. Chem.* **1980**, *16*, 207.

(26) Yamada, F.; Slagle, I. R.; Gutman, D. *Chem. Phys. Lett.* **1981**, *83*, 409.

(27) Park, J.-Y.; Gutman, D. *J. Phys. Chem.* **1983**, *87*, 1844.

(28) Slagle, I. R.; Yamada, F.; Gutman, D. *J. Am. Chem. Soc*. **1981**, *103*, 149.

(29) Loewenstein, L. M.; Anderson, J. G. *J. Phys. Chem.* **1987**, *91*, 2993.

(30) Paltenghi, R.; Ogryzlo, E. A.; Bayes, K. D. *J. Phys. Chem.* **1984**, *88*, 2595.

(31) Timonen, R. S.; Seetula, J. A.; Niiranen, J.; Gutman, D. *J. Phys. Chem.* **1991**, *95*, 4009.

(32) Seetula, J. A.; Gutman, D.; Lightfoot, P. D.; Rayes, M. T.; Senkan, S. M. *J. Phys. Chem.* **1991**, *95*, 10688.

(33) Abbatt, J. P. D.; Anderson, J. G. *J. Phys. Chem.* **1991**, *95*, 2382.

(34) Oakes, J. M.; Ellison, G. B. *J. Am. Chem. Soc*. **1983**, *105*, 2969.

(35) Geppert, W. D.; Eskola, A. J.; Timonen, R. S.; Halonen, L. *J. Phys. Chem. A* **2004**, *108*, 4232.

(36) Clary, D. C. *Annu. Rev. Phys. Chem.* **1990**, *41*, 61.

(37) Mozurkewich, M.; Benson, S. W. *J. Phys. Chem.* **1984**, *88*, 6429.

(38) Russell, J. J.; Seetula, J. A.; Timonen, R. S.; Gutman, D.; Nava, D. F. *J. Am. Chem. Soc.* **1988**, *110*, 3084.